The relationship between the seismic bending moment of pier bottom and the initial lifting bending moment of railway self-centering pier

Zhijie Zhu*, Xiushen Xia, Haoran Zhu, Xin Qiao, Heng Zhang and Xudong Zhang

School of Civil Engineering, Lanzhou Jiaotong University, Lanzhou, Gansu, 730070, China

*Corresponding author's e-mail:1621471818@qq.com

Abstract. In order to explore the relationship between the maximum seismic bending moment at the bottom of a railway self-repositioning pier and its initial lifting moment, a finite element analysis model is established based on OpenSees platform on a 32m railway simple supported beam bridge as the engineering background, and 300 seismic waves are input, among which 251 seismic waves cause the structure to lift away. The relationship between the ratio of the maximum seismic bending moment and the initial lifting bending moment at the bottom of the pier under 251 seismic waves and the peak acceleration of the input ground motion is obtained, and the data is fitted by polynomial function. The results show that the maximum seismic bending moment at the bottom of the pier increases with the increase of the peak seismic acceleration, and the theoretical formula of the dynamic magnification factor β of the bending moment at the bottom of the railway self-repositioning pier when the pier is lifted from the rock under strong earthquake has high accuracy. The research results can provide some theoretical reference for seismic design of self-resetting pier.

Keywords: Railway; Self-centering pier; Seismic bending moment; Initial lifting moment; Numerical fitting.

1 Introduction

With the gradual deepening of seismic research, the research of self-resetting pier has gradually become the focus of research. Compared with ordinary pier, self-resetting pier has superior seismic performance and better application prospects.

In recent years, many scholars have carried out a lot of research on self-resetting pier.Zhang Zhexi et al[1] proposed a self-resetting pier using superelastic shape memory alloy (SMA) cable, and conducted nonlinear time-history curve analysis through OpenSees platform. The results show that the pier using SMA cable can effectively reduce the residual deformation of the structure and the damage of the pier itself. Shao Shu [2] proposed a self-resetting pier with SMA rod and analyzed its seismic performance. The results show that the SMA rod has good self-resetting performance and the maximum displacement of the pier top has been significantly im-

P. Xiang et al. (eds.), *Proceedings of the 2023 5th International Conference on Hydraulic, Civil and Construction Engineering (HCCE 2023)*, Atlantis Highlights in Engineering 26,
https://doi.org/10.2991/978-94-6463-398-6_43

proved. Xia Xiuden et al. studied the technology of pier bottom isolation [3], compared the mechanism and effect of rocking isolation with that of bearing absorption, and pointed out the advantages of high efficiency and stability of rocking isolation, and found that the maximum bending moment of rocking isolation pier was basically unaffected by the spectral characteristics of ground motion [4]. Subsequently, various high pier rocking isolation models were compared, and the method of lifting spring stiffness was given. The accuracy of the models was verified by combining pseudo-static test and finite element simulation. The influence of the limiting device on the seismic response of self-relocating pier, pier bottom bending moment, etc., was investigated, and the accuracy of various high pier rocking isolation models was compared [5]. The influencing factors of pier bottom bending moment [6] are also pointed out. Wei Xinghan [7] conducted a pseudo-static test of self-resetting pier to explore the influence of limiting reinforcement on the response of lifting condition, lifting Angle, pier bottom bending moment and compression zone width of self-resetting pier. Tang Jingyao [8] studied the effect of ground motion strength, characteristics and limiting reinforcement on dynamic response of self-resetting pier. Shi Jun [9] conducted pseudo-static tests on self-resetting piers with sacrificative components, studied the energy dissipation capacity, lateral displacement stiffness and seismic mechanism of self-resetting piers with sacrificative components, and pointed out that the existence of sacrificative components limited the pier bottom slip, pier bottom lift and pier bottom Angle of self-resetting piers, and increased the energy dissipation capacity of self-resetting piers.Ma Huajun [10] carried out quasi-static test and shaking table test of rocking isolation pier at the same time, compared the isolation mechanism of rocking isolation pier, rocking pier with energy-dissipating steel bars and rocking pier with anti-overturning steel bars, established its finite element model through OpenSees, and proposed the design method and principle of rocking isolation pier. Palermo et al. [11] carried out a pseudo-static experiment of prestressed segment prefabricated rectangular piers, and found that: compared with bonded prestressed tendons, unbonded prestressed tendons can reduce the damage of piers and have significant self-resetting effect. EI-Gawdy et al. [12] studied the influence of energy-dissipating components in self-repositioning piers on the seismic performance of piers, and found that energy-dissipating components both improved the ductility performance and energy-dissipating capacity of piers, and could reduce the residual strain of piers. Trono et al. [13] studied the fiber concrete hollow monolithic self-resetting pier and found that the seismic performance of the pier was similar to that of the traditional pier, but it was easier to replace after an earthquake. The seismic bending moment at the bottom of self-resetting pier is less affected by seismic spectrum and less obvious with the increase of seismic intensity, which depends on two factors: 1) the initial lifting moment of the rock; 2) Dynamic amplification factor of pier bottom bending moment caused by rocking vibration. However, the above article did not carry out this research.

In this paper, a numerical analysis model of railway self-resetting pier is established based on OpenSees platform, and the relationship between the initial lifting bending moment, the maximum seismic bending moment at the bottom of pier and the peak acceleration of input ground motion is discussed by inputting 300 strong earthquake

records. The research results can provide theoretical support for the design of self-resetting pier.

2 Calculation of initial lifting moment of self-resetting pier

2.1 Self-resetting pier structure

According to literature [6], the earthquake isolation mechanism of self-resetting pier is as follows: when the bottom bending moment of pier exceeds the anti-overturning bending moment provided by the structure itself, the structure will be lifted, consume energy through its own swaying, and realize complete self-resetting through its own weight after an earthquake, as shown in Figure 1.

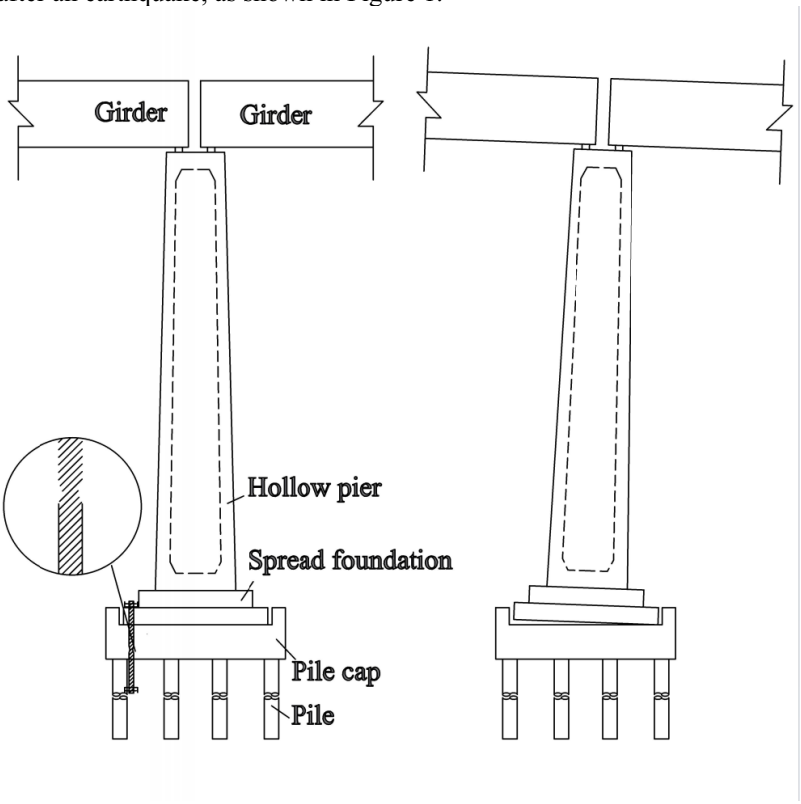

(a) The adhesion stage (b) The swing phase

Fig. 1. Schematic diagram of self resetting bridge pier structure.

2.2 Calculation of initial lifting bending moment of self-resetting pier

The initial lifting bending moment of self-resetting pier is shown in Figure 2, which can be calculated according to formula (1) [6]:

$$M_y = F \cdot H = (N + G) \cdot \frac{B}{2} \tag{1}$$

Where N is the reaction force of the bridge across the top of the pier, G is the weight of the pier itself, and B represents the width of the foundation expanded by the calculation direction connected with the pier.

The content of this paper is to study the relationship between the maximum seismic bending moment Me and the initial lifting moment My at the bottom of self-resetting pier after the structure is lifted off under the action of ground motion.

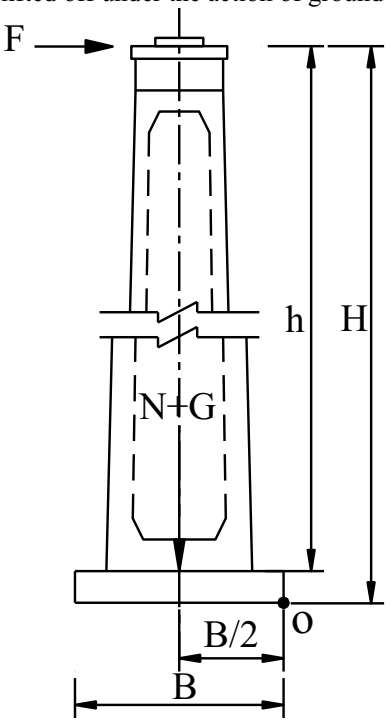

Fig. 2. Calculation diagram of initial lifting moment.

3 Establishment of finite element analysis model

3.1 Basic analysis data

The calculation example data used in this paper is a single track railway bridge in literature [6], as shown in Figure 3. Taking Pier No. 18 as the research object, the traditional pier No. 18 is redesigned to be a self-resetting pier. The expanded foundation of the pier bottom after redesign is C30 concrete, the width B=10m, and the cross-sectional area A0=120m^2. The sum of the vertical force under constant load at the bottom of the pier is 33873kN. According to formula (1), it can be seen that My=33873×10/2=169365kNm.

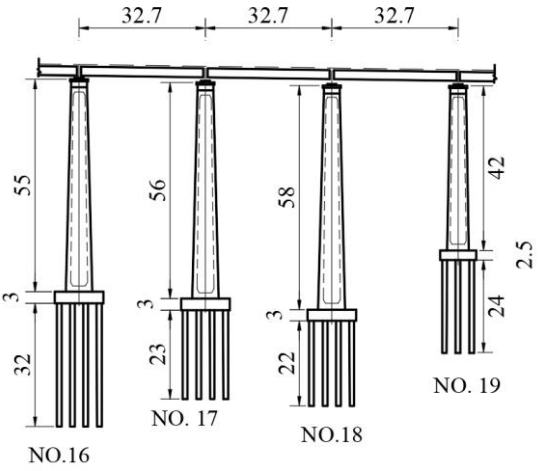

Fig. 3. Facade Layout of a High Pier Bridge on a Railway.

3.2 Model Establishment

A free-swinging two-spring model was adopted, as shown in FIG. 4, in which the simulation methods of pier column, span mass and pier lifting in literature [6] were adopted. The element elastic Beam Column was used to simulate the pier column, and the rigid arm element was used to simulate the pier bottom to expand the foundation. The rigid arm stiffness was 100 times of the maximum stiffness of the element. The lifting of piers is simulated by the compression spring only. The lifting spring is simulated by the zero-length element zeroLength, and the material constitutive relationship is simulated by the elastic compression material uniaxialMaterialENT. According to literature [5], the lifting spring stiffness k of pier bottom is 2.1×108kN/m.

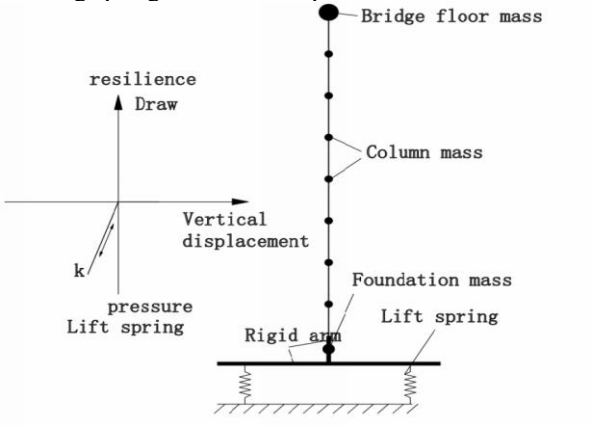

Fig. 4. Analysis model of self resetting high pier.

4 Calculation results and analysis

4.1 Result of time history analysis

300 seismic waves were selected from the US Pacific Strong Earthquake Database (PEER), and some of the wave information is listed in Table 1. The original seismic waves are directly fed into the OpenSees model, and there are 251 seismic waves that cause the structure to shake off. The results of some data (80 items) are shown in Table 2. The relationship between the maximum seismic bending moment Me at the bottom of 251 piers under ground motion, the initial lifting bending moment My and the maximum peak acceleration PGA of ground motion is shown in Figure 5. The ratio of the average value of the maximum seismic bending moment at the bottom of 251 piers under seismic waves to the initial lifting bending moment My is about 1.22.

Table 1. Input Ground Motion Information.

Serial number	ID	Earthquake name	station	Earthquake magnitude	Epicentral distance(km)	Recorded components of strong earthquakesPGA(g)
1	1	Helena_ Montana-01	Carroll College	6.0	2.86	0.406
2	3	Humbolt Bay	Ferndale City Hall	5.8	71.57	0.297
3	17	Southern Calif	San Luis Obispo	6.0	73.41	0.254
4	178	Imperial Valley-06	El Centro Array #3	6.5	6.63	0.235
5	179	Imperial Valley-06	El Centro Array #4	6.5	7.05	0.269
6	180	Imperial Valley-06	El Centro Array #5	6.5	3.95	0.375
7	181	Imperial Valley-06	El Centro Array #6	6.5	1.35	0.352
8	292	Irpinia_ Italy-01	Sturno (STN)	6.9	10.84	0.236
9	180	Darfield_ New Zealand	TPLC	7.0	6.11	0.299
10	185	Imperial Valley-06	Holtville Post Office	6.9	3.85	0.257
11	767	Loma Prieta	Gilroy Array #3	6.9	12.82	0.288
12	764	Loma Prieta	Saratoga - Aloha Ave	6.9	8.5	0.308
13	8161	El Mayor-Cucapah_ Mexico	El Centro Array #12	7.2	11.26	0.251
14	8606	El Mayor-Cucapah_ Mexico	Westside Elementary School	7.2	11.44	0.307
15	1013	Northridge-01	LA Dam	6.7	11.34	0.319
16	174	Imperial Valley	Brawley Airport	6..5	12.56	0.367
17	1487	Chi-Chi_ Taiwan	TCU047	7.6	35	0.292
18	1491	Imperial Valley-06	Agrarias	6.5	0.65	0.287
19	1510	Chi-Chi_ Taiwan	TCU075	7.1	5.76	0.233
20	3746	Cape Mendocino	Centerville Beach_ Naval Fac	7.0	18.31	0.318
21	4847	Chuetsu-oki_ Japan	Joetsu Kakizakiku Kakizaki	6.8	11.94	0.450
22	6927	Darfield_ New Zealand	LINC	7.0	7.11	0.388
23	1161	Kocaeli_ Turkey	Gebze	7.5	10.92	0.261
24	1165	Kocaeli_ Turkey	Izmit	7.5	7.21	0.230
25	1176	Kocaeli_ Turkey	Yarimca	7.5	4.83	0.232
26	1182	Chi-Chi_ Taiwan	CHY006	7.6	9.76	0.359
27	1244	Chi-Chi_ Taiwan	CHY101	7.6	9.94	0.333
28	1511	Chi-Chi_ Taiwan	TCU076	7.6	2.74	0.283
29	2734	Chi-Chi_ Taiwan-04	CHY074	6.2	6.2	0.284
30	3473	Chi-Chi_ Taiwan-06	TCU078	6.3	11.52	0.266
31	4458	Montenegro_ Yugoslavia	Ulcinj - Hotel Olimpic	7.1	5.76	0.424
32	4483	L'Aquila_ Italy	L'Aquila - Parking	6.3	5.38	0.335
33	6897	Darfield_ New Zealand	DSLC	7	8.46	0.257
34	6928	Darfield_ New Zealand	LPCC	7	25.67	0.258
35	6959	Darfield_ New Zealand	Christchurch Resthaven	7	19.48	0.237

Table 2. Relationship between the ratio of maximum seismic bending moment to initial uplift bending moment at the pier bottom and the peak ground acceleration

Earthquake			Earthquake			Earthquake			Earthquake		
Serial number	PGA/g	Me/My	Serial number	PGA/g	M_e/M_y	Serial number	PGA/g	Me/My	Serial number	PGA/g	Me/My
1	0.406	1.258	21	0.450	1.341	41	0.246	1.172	61	0.255	1.177
2	0.297	1.194	22	0.388	1.243	42	0.246	1.172	62	0.256	1.178
3	0.254	1.177	23	0.261	1.181	43	0.247	1.173	63	0.256	1.179
4	0.235	1.162	24	0.230	1.156	44	0.248	1.174	64	0.257	1.179
5	0.269	1.185	25	0.232	1.160	45	0.249	1.174	65	0.258	1.179
6	0.375	1.216	26	0.359	1.202	46	0.250	1.175	66	0.259	1.180
7	0.252	1.176	27	0.333	1.191	47	0.251	1.176	67	0.260	1.180
8	0.236	1.163	28	0.283	1.189	48	0.252	1.176	68	0.261	1.181
9	0.299	1.194	29	0.284	1.189	49	0.278	1.187	69	0.286	1.190
10	0.257	1.179	30	0.266	1.183	50	0.279	1.188	70	0.286	1.191
11	0.288	1.191	31	0.424	1.279	51	0.280	1.188	71	0.287	1.191
12	0.308	1.196	32	0.335	1.190	52	0.281	1.189	72	0.288	1.191
13	0.251	1.176	33	0.257	1.179	53	0.282	1.189	73	0.289	1.191
14	0.307	1.196	34	0.258	1.179	54	0.283	1.189	74	0.290	1.191
15	0.319	1.185	35	0.237	1.187	55	0.284	1.189	75	0.291	1.192
16	0.367	1.195	36	0.278	1.187	56	0.285	1.189	76	0.292	1.192
17	0.292	1.192	37	0.371	1.211	57	0.371	1.211	77	0.373	1.213
18	0.287	1.191	38	0.375	1.217	58	0.376	1.217	78	0.377	1.219
19	0.233	1.160	39	0.378	1.223	59	0.379	1.224	79	0.380	1.227
20	0.318	1.196	40	0.382	1.231	60	0.383	1.233	80	0.384	1.236

4.2 Result fitting

As can be seen from FIG. 5, when the structure is lifted, the maximum seismic bending moment at the bottom of the pier also shows an overall trend of increasing with the gradual increase of the peak acceleration of seismic waves, and the two show a certain relationship.

The polynomial function was used to perform numerical fitting of the calculation results, and the relationship between the ratio of the maximum seismic bending moment Me at the bottom of the pier and the initial lifting bending moment My and the peak acceleration of ground motion was obtained, as shown in equation (2).

$$\begin{gathered}\beta = -207.9a^4 + 324.2a^3 - 179.8a^2 + 42.8a - 2.6 \\ 0.227g < a < 0.45g\end{gathered} \tag{2}$$

Where, β represents the ratio of the maximum seismic bending moment Me at the bottom of the pier to the initial lifting bending moment My, that is, the dynamic amplification factor of the initial lifting bending moment caused by rocking vibration, and a represents the peak acceleration of the seismic wave.

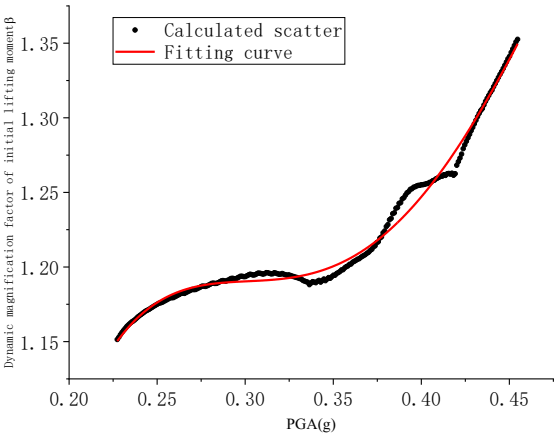

Fig. 5. calculates the scatter-to-function fitting curve.

It can also be seen from Figure 5 that the degree of fitting of the calculated results is high, and the correlation coefficient r^2=0.9894, which also verifies the reliability of this function to a certain extent. Therefore, formula (2) can be used to calculate the dynamic amplification factor of the bottom moment of the pier after the structure is lifted.

4.3 Formula Verification

Another 30 seismic waves were selected again from the Pacific Earthquake Center to verify equation (2). The ratio β of the maximum seismic bending moment at the bottom of the pier to the initial lifting moment obtained from the time history analysis and the calculated values of the formula are listed in Table 3.

Table 3. Comparison of fitting results and time history calculation results

Earthquake		β		error%
Number	PGA(g)	actual result	Formula result	
252	0.299	1.141	1.127	1.2
253	0.300	1.143	1.127	1.3
254	0.301	1.144	1.127	1.5
255	0.302	1.146	1.127	1.6
256	0.303	1.148	1.127	1.8
257	0.304	1.150	1.127	2.0
258	0.305	1.152	1.127	2.2
259	0.306	1.154	1.127	2.3
260	0.307	1.156	1.127	2.5

261	0.308	1.158	1.127	2.6
262	0.309	1.160	1.127	2.8
263	0.310	1.161	1.127	2.9
264	0.311	1.162	1.127	3.1
265	0.312	1.163	1.127	3.3
266	0.313	1.167	1.128	3.4
267	0.314	1.169	1.128	3.5
268	0.315	1.171	1.128	3.9
269	0.316	1.173	1.128	3.8
270	0.317	1.174	1.128	4.0
271	0.318	1.176	1.128	4.1
272	0.319	1.178	1.128	4.2
273	0.320	1.179	1.128	4.4
274	0.321	1.181	1.128	4.5

As can be seen from Table 3, the error between the actual calculation results and the formula results is between 1.2% and 5.3%, which indicates that the formula given in the paper has a high accuracy when used to calculate the maximum seismic bending moment at the bottom of the pier.

5 Conclusion

In this paper, a finite element model of self-resetting pier is established based on OpenSees platform, and 300 strong earthquake records are input to explore the relationship between the maximum seismic bending moment at the bottom of pier and the initial lifting bending moment. The following conclusions are drawn:

In this paper, a finite element model of self-resetting pier is established based on OpenSees platform, and 300 strong earthquake records are input to explore the relationship between the maximum seismic bending moment at the bottom of pier and the initial lifting bending moment. The following conclusions are drawn:

(1) By numerical fitting of polynomial function, a theoretical formula for calculating the dynamic magnification factor β of the bottom bending moment of railway self-resetting pier when it is lifted away from the swaying pier under strong earthquake is given.

(2) When the self-repositioning pier is removed, the dynamic magnification factor β of the pier bottom bending moment has a certain correlation with the peak acceleration of the input seismic wave.

When the peak acceleration of the seismic wave is between 0.227g and 0.45g, the ratio of the average maximum seismic moment at the bottom of the pier to the initial lifting moment is about 1.22.

References

1. Zhang Zhexi, Liang Dong, Fang Cheng, et al. Experimental research and dynamic analysis of rocking self-resetting pier with SMA cable [J]. World Earthquake Engineering,2020, 36(04): 138-146.
2. Shao Shu Research on seismic performance of self resetting bridge piers with SMA poles [D] Chang'an University, 2019
3. Xia Xiushen Research on Seismic Design Method for Railway High Piers [D] Lanzhou Jiaotong University, 2012
4. Xia Xiushen, Chen Xingchong. A comparative study on vibration isolation of base and pier top for railway high-pier Bridges [J]. Journal of Railway Sciences,2011, 33(09): 102-107.
5. Xia Xiushen, Chen Xingchong. Research on Vibration Isolation Analysis Model of pile Foundation High Pier [J]. Journal of Railways, 2013,41(10): 1470-1475.
6. Xia Xiushen, Chen Xingchong, Li Jianzhong. Self-resetting isolation mechanism of high pier [J]. Journal of Central South University (Natural Science Edition), 2015, 46 (07): 2549-2557.
7. Wei Xinghan. Quasi-static test of self-resetting isolation high pier Model [D]. Lanzhou Jiaotong University, 2018.
8. TANG Jingyao. Shaking Table Test of Self-resetting High Pier Model [D]. Lanzhou Jiaotong University, 2018.
9. SHI Jun. Quasi-static Test Research of self-resetting Pier with sacrificial Parts [D]. Lanzhou Jiaotong University,2021.
10. Ma Huajun. Research on Vibration Isolation Mechanism and seismic Design Method of railway pile Foundation pier [D]. Lanzhou Jiaotong University,2019.
11. Palermo A, Pampanin S, Calvi G M. Concept and development of hybrid solutions for seismic resistant bridge systems [J]. Journal of Earthquake Engineering, 2005, 9(6): 899-921.
12. EIGawdy M A, shalan A. Seismic behavior of self-centering precast segmental bridge bents[J]. Journal of bridge Engineering,2014,16(3):328-339.
13. Nguyen W, Trono W, Panagiotou M, et al. Seismic response of a rocking bridge column using a precast hybrid fiber-reinforced concrete (HyFRC)tube[J]. Composite Structures, 2017,174:252-262.